

Aspirin-inspired acetyl-donating HDACs inhibitors

Jiah Lim¹ · Yoojin Song¹ · Jung-Hee Jang² · Chul-Ho Jeong¹ · Sooyeon Lee¹ ·
Byoungduck Park¹ · Young Ho Seo¹ 

Received: 13 March 2018 / Accepted: 4 June 2018 / Published online: 20 June 2018
© The Pharmaceutical Society of Korea 2018

Abstract Aspirin is one of the oldest drugs for the treatment of inflammation, fever, and pain. It is reported to covalently modify COX-2 enzyme by acetylating a serine amino acid residue. By virtue of aspirin's acetylating potential, we for the first time developed novel acetyl-donating HDAC inhibitors. In this study, we report the design, synthesis, in silico docking study, and biological evaluation of acetyl-donating HDAC inhibitors. The exposure of MDA-MB-231 cells with compound **4c** significantly promotes the acetylation of α -tubulin and histone H3, which are substrates of HDAC6 and HDAC1, respectively. In silico docking simulation also indicates that compound **4c** tightly binds to the deep substrate-binding pocket of HDAC6 by coordinating the active zinc ion in a bidentate manner and forming hydrogen bond interactions with Ser531 and His573 amino acid residues. In particular, compound **4c** ($GI_{50} = 147 \mu\text{M}$) affords the significant enhancement of anti-proliferative effect on MDA-MB-231 cells, compared with its parent compound **2c** ($GI_{50} > 1000 \mu\text{M}$) and acetyl-donating group deficient compound **6** ($GI_{50} = 554 \mu\text{M}$). Overall, compound **4c** presents a novel strategy for developing acetyl-donating HDAC inhibitors.

Keywords Aspirin · Histone deacetylases · Cancers · Alzheimer's disease · Drug addiction

Introduction

Histone deacetylases (HDACs) have emerged as important pharmaceutical targets for a wide range of diseases, including cancer, Alzheimer's disease, depression, and drug addiction (Kazantsev and Thompson 2008; Cuadrado-Tejedor et al. 2017; D'ydwalle et al. 2012; Golden et al. 2013; Omonijo et al. 2014; Chun 2018). The reversible acetylation of lysine residues at the *N*-terminal tails of core histones has a critical role in epigenetic regulation of gene expression. This acetylation status is tightly regulated by the balance of HDACs and histone acetyltransferases (HATs) and the perturbation of this balance is closely linked to the onset and progression of many diseases (Hong et al. 1993; Ropero and Esteller 2007). Therefore, the inhibition of HDACs helps in restoring the aberrant epigenetic changes associated with diverse disorders (Bolden et al. 2006; Kazantsev and Thompson 2008). HDACs catalyze the removal of ϵ -*N*-acetyl groups from lysine residues at the *N*-terminal tails of core histones, impeding the accessibility of transcriptional factors to promoter segments of DNA within the condensed chromatin (Lee et al. 1993). HDACs substrates are not limited to histone proteins. These enzymes also regulate the acetylation levels of non-histone proteins such as α -tubulin, Hsp90, p53, c-Myc, NF- κ B, and E2P (Glozak et al. 2005). HDAC inhibitors are commonly classified into four main classes based on their chemical structure, hydroxamic acids, benzamides, cyclic peptides, and short-chain fatty acids (Nebbio et al. 2012). To date, the U.S FDA has approved four HDAC inhibitors as anticancer drugs and these include

Jiah Lim and Yoojin Song contributed equally to this work.

✉ Young Ho Seo
seoyho@kmu.ac.kr

¹ College of Pharmacy, Keimyung University, Daegu 42601, Republic of Korea

² Department of Pharmacology, School of Medicine, Keimyung University, Daegu 42601, Republic of Korea

SAHA (vorinostat) (Duvic et al. 2007), FK-228 (romidepsin) (VanderMolen et al. 2011), PXD101 (belinostat) (Lee et al. 2015), and LBH589 (panobinostat) (Raedler 2016), while HBI-8000 (chidamide) (Lu et al. 2016) has been approved by the Chinese FDA for the treatment of cutaneous T cell lymphoma (Fig. 1). Although most HDAC inhibitors have been primarily developed for the hematological malignancies (Tambaro et al. 2010), an increasing number of HDAC inhibitors are recently investigated for the treatment of central nervous system (CNS) diseases such as Alzheimer's disease, depression, and drug addiction (Kazantsev and Thompson 2008).

Aspirin (acetylsalicylic acid) is one of the oldest and most widely used drugs for the treatment of inflammation, fever, and pain as well as for the prevention of cardiovascular diseases. Like many other nonsteroidal anti-inflammatory drugs (NSAIDs), its basic mechanism of action as an anti-inflammatory drug is well documented to target cyclooxygenase-2 (COX-2). More specifically, aspirin is reported to covalently modify COX-2 through acetylation of Ser530 near its active site, which prevents its native substrate from properly binding to its active site (Lei et al. 2015).

In recent years, epidemiological data and accumulating scientific evidence have shown that aspirin can also reduce overall risk of various types of cancers (Patrignani and Patrono 2016). Although the precise mechanisms exerting its anticancer effects are not yet clearly elucidated, newly report suggests that aspirin's ability to chemically acetylate endogenous proteins has immense therapeutic significance in cancers (Sonnemann et al. 2008). The unique acetylating nature of aspirin intrigues us to investigate anticancer effect of aspirin analogues and their therapeutic potential as HDAC inhibitors.

Materials and methods

Chemistry

Unless otherwise noted, all reactions were performed under argon atmosphere in oven-dried glassware. All purchased reagents and solvents were used without further purification. Thin layer chromatography (TLC) was carried out using Merck silica gel 60 F₂₅₄ plates. TLC plates were visualized using a combination of UV, p-anisaldehyde, ceric ammonium molybdate, ninhydrin, and potassium permanganate staining. Column chromatography was conducted under medium pressure on silica (Merck Silica Gel 40–63 μm) or performed by MPLC (Biotage Isolera One instrument) on a silica column (Biotage SNAP HP-Sil) or C18 column (Biotage SNAP Ultra C18). NMR analyses were carried out using a JNM-ECZ500R (500 MHz) manufactured by Jeol resonance. ¹H and ¹³C NMR chemical shifts are reported in parts per million (ppm). The deuterium lock signal of the sample solvent was used as a reference, and coupling constants (*J*) are given in hertz (Hz). The splitting pattern abbreviations are as follows: s, singlet; d, doublet; t, triplet; q, quartet; dd, doublet of doublets; m, multiplet. The purity of all tested compounds was confirmed to be higher than 95% by analytical HPLC performed with a dual pump Shimadzu LC-6AD system equipped with VP-ODS C18 column (4.6 mm × 250 mm, 5 μm, Shimadzu).

3-Acetoxybenzoic acid (2b)

A mixture of 3-hydroxybenzoic acid (1.0 g, 138.12 mmol) and acetic anhydride (5 mL) in pyridine (10 mL) was stirred at 125 °C for 2 h, equipped with a refluxing condenser under argon. After cooling at room temperature, the

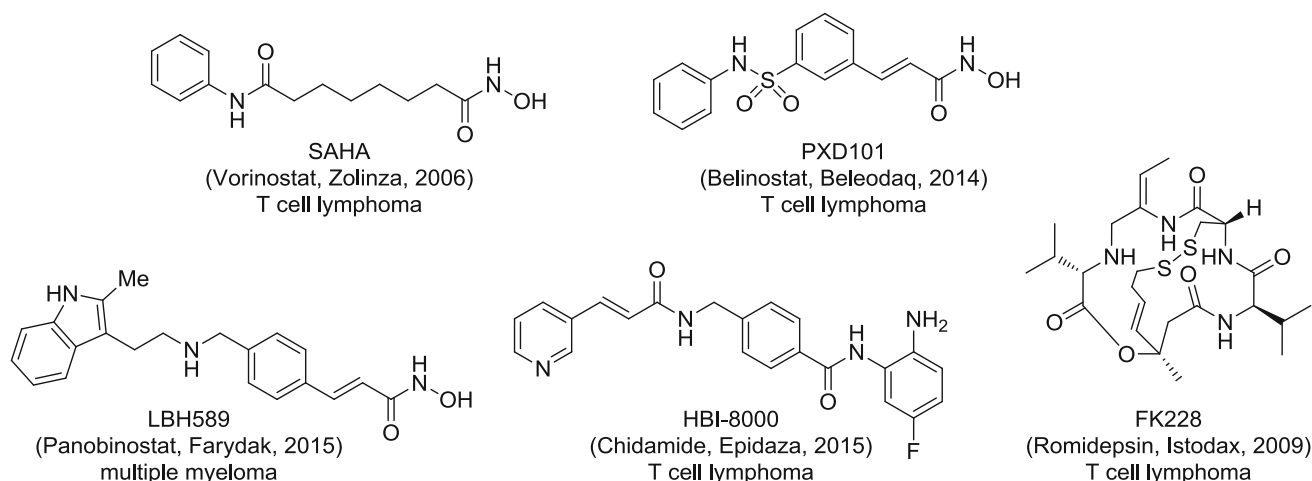


Fig. 1 Structures of FDA-approved HDAC inhibitors

mixture was quenched with saturated aqueous NaHCO₃, acidified with 12 *N* HCl to pH 2. The resulting solid was filtered, washed with H₂O (50 mL), and dried under high vacuum to afford compound **2b** in 94% yield. ¹H NMR (500 MHz, CDCl₃) δ 7.99 (d, *J* = 8.0 Hz, 1H), 7.83 (s, 1H), 7.50 (t, *J* = 8.0 Hz, 1H), 7.37–7.34 (m, 1H), 2.34 (s, 3H). ¹³C NMR (125 MHz, CDCl₃) δ 171.1, 169.3, 150.7, 130.8, 129.7, 127.7, 127.3, 123.5, 21.1. ESI MS (*m/e*) = 179.03 [M-1]⁻.

4-(Hydroxycarbamoyl)phenyl acetate (2c)

A mixture of 4-hydroxybenzoic acid (1.0 g, 138.12 mmol) and acetic anhydride (5 mL) in pyridine (10 mL) was stirred at 125 °C for 2 h, equipped with a refluxing condenser under argon. After cooling at room temperature, the mixture was quenched with saturated aqueous NaHCO₃, acidified with 12 *N* HCl to pH 2. The resulting solid was filtered, washed with H₂O (50 mL), and dried under high vacuum to afford compound **2c** in 66% yield. ¹H NMR (500 MHz, CDCl₃) δ 8.14 (d, *J* = 8.6 Hz, 2H), 7.21 (d, *J* = 8.6 Hz, 2H), 2.34 (s, 3H). ¹³C NMR (125 MHz, CDCl₃) δ 171.0, 169.0, 155.0, 131.9, 126.9, 121.9, 21.3. ESI MS (*m/e*) = 179.03 [M-1]⁻.

2-((Benzyloxy)carbamoyl)phenyl acetate (3a)

A mixture of compound **2a** (0.2 g, 1.11 mmol), *o*-benzylhydroxylamine hydrochloride (0.19 g, 1.22 mmol), EDC (0.43 g, 2.22 mmol), and DIPEA (0.39 mL, 2.22 mmol) in DCM (25 mL) was stirred at room temperature for 4 h. The reaction mixture was diluted with DCM (100 mL) and washed with 1 *N* HCl (100 mL) and then with brine (100 mL), dried over Na₂SO₄, concentrated under reduced pressure and purified by silica gel column chromatography to afford compound **3a** in 71% yield. *R*_f = 0.32 (4:6 ethyl acetate: hexane). ¹H NMR (500 MHz, CDCl₃) δ 8.63 (s, 1H), 7.73 (d, *J* = 7.4 Hz, 1H), 7.50–7.44 (m, 3H), 7.39 (q, *J* = 7.3 Hz, 3H), 7.29 (t, *J* = 7.7 Hz, 1H), 7.09 (d, *J* = 8.0 Hz, 1H), 5.03 (s, 2H), 2.10 (s, 3H). ¹³C-NMR (125 MHz, CDCl₃) δ 169.0, 164.1, 148.1, 135.4, 132.6, 130.0, 129.3, 128.9, 128.8, 126.4, 125.3, 123.3, 78.2, 20.94. ESI MS (*m/e*) = 286.11 [M + 1]⁺.

3-((Benzyloxy)carbamoyl)phenyl acetate (3b)

A mixture of compound **2b** (0.2 g, 1.11 mmol), *o*-benzylhydroxylamine hydrochloride (0.19 g, 1.22 mmol) with DIPEA (0.39 mL) in DCM (25 mL) was stirred by EDC (0.43 g, 2.22 mmol) at room temperature for 4 h. The mixture was diluted in DCM (100 mL). The organic layer was washed with 1 *N* HCl (100 mL) twice and then with brine (100 mL), dried over Na₂SO₄, concentrated under

reduced pressure to afford compound **3b** in 68% yield. ¹H NMR (500 MHz, CDCl₃) δ 8.82 (s, 1H), 7.49 (d, *J* = 7.4 Hz, 1H), 7.43 (m, 3H), 7.41–7.36 (m, 4H), 7.22 (d, *J* = 7.4 Hz, 1H), 5.01 (s, 2H), 2.29 (s, 3H). ¹³C NMR (125 MHz, CDCl₃) δ 169.4, 165.4, 150.7, 135.2, 133.5, 129.8, 129.4, 128.9, 128.7, 128.4, 127.9, 125.4, 124.5, 120.8, 78.4, 21.1. ESI MS (*m/e*) = 286.11 [M + 1]⁺.

4-((Benzyloxy)carbamoyl)phenyl acetate (3c)

A mixture of compound **2c** (0.2 g, 1.11 mmol), *o*-benzylhydroxylamine hydrochloride (0.19 g, 1.22 mmol), DIPEA (0.39 mL) in DCM (25 mL) was stirred with EDC (0.43 g, 2.22 mmol) at room temperature for 4 h. The mixture was diluted in DCM (100 mL). The organic layer was washed with 1 *N* HCl (100 mL) twice and then with brine (100 mL), dried over Na₂SO₄, concentrated under reduced pressure to afford compound **3c** in 60% yield. ¹H NMR (500 MHz, CDCl₃) δ 7.69 (d, *J* = 8.6 Hz, 2H), 7.41–7.40 (m, 2H), 7.37–7.33 (m, 3H), 7.08 (d, *J* = 8.6 Hz, 2H), 4.98 (s, 2H), 2.29 (s, 3H). ¹³C NMR (125 MHz, CDCl₃) δ 169.1, 165.7, 153.5, 135.3, 129.6, 129.4, 128.9, 128.7, 128.4, 122.0, 121.6, 78.4, 21.2. ESI MS (*m/e*) = 286.11 [M + 1]⁺.

3-(Hydroxycarbamoyl)phenyl acetate (4b)

A mixture of compound **3b** (0.203 g, 1.04 mmol) and Pd/C (0.05 g) in MeOH (12.5 mL) was stirred at room temperature for 2 h under hydrogen. The resulting mixture was diluted in MeOH (50 mL), filtered, and concentrated under reduced pressure, and purified by MPLC (Biotage SNAP HP-Sil column) to afford compound **4b** in 45% yield. *R*_f = 0.31 (7:3 ethyl acetate: hexane). ¹H NMR (500 MHz, acetone-d₆) δ 7.71 (d, *J* = 8.0 Hz, 1H), 7.57 (s, 1H), 7.50 (t, *J* = 7.7 Hz, 1H), 7.30–7.28 (m, 1H), 2.28 (s, 3H). ¹³C NMR (125 MHz, acetone-d₆) δ 169.6, 164.8, 151.9, 134.6, 130.3, 130.1, 125.8, 124.8, 121.5, 20.9. ESI MS (*m/e*) = 194.08 [M-1]⁻.

4-(Hydroxycarbamoyl)phenyl acetate (4c)

A mixture of compound **3c** (0.203 g, 1.04 mmol) and Pd/C (0.05 g) in MeOH (12.5 mL) was stirred at room temperature for 2 h under hydrogen. The resulting mixture was dissolved in MeOH (50 mL), filtered, and concentrated under reduced pressure, and purified by MPLC (Biotage SNAP HP-Sil column) to afford compound **4c** in 39% yield. *R*_f = 0.24 (7:3 ethyl acetate: hexane). ¹H NMR (500 MHz, acetone-d₆) δ 10.8 (s, 1H), 8.52 (s, 1H), 7.88 (d, *J* = 8.0 Hz, 2H), 7.22 (d, *J* = 8.0 Hz, 2H), 2.28 (s, 3H). ¹³C NMR (125 MHz, acetone-d₆) δ 168.6, 164.5, 153.5, 129.7, 128.4, 122.0, 20.2. ESI MS (*m/e*) = 194.08 [M-1]⁻.

4-Hydroxy-*N*-((tetrahydro-2H-pyran-2-yl)oxy)benzamide (**5**)

A mixture of 4-hydroxybenzoic acid (1.0 g, 7.24 mmol), *o*-(Tetrahydro-2H-pyran-2-yl) hydroxylamine (0.93 g, 7.96 mmol), and EDC (2.78 g, 14.48 mmol) in DMF (25 mL) was stirred by at room temperature for 12 h. The resulting mixture was dissolved in DCM (100 mL). The organic layer was washed with 1 *N* HCl (100 mL) and then washed with brine (100 mL), dried over Na₂SO₄, concentrated under reduced pressure and purified by silica gel column chromatography to afford compound **5** in 22% yield. *R*_f = 0.53 (7:3 ethyl acetate: hexane). ¹H NMR (500 MHz, DMSO-*d*₆) δ 11.4 (s, 1H), 10.1 (s, 1H), 7.63 (d, *J* = 8.6 Hz, 2H), 6.80 (d, *J* = 9.2 Hz, 2H), 4.94 (s, 1H), 4.06–4.02 (m, 1H), 3.51–3.48 (m, 1H), 1.70–1.53 (m, 6H). ¹³C NMR (125 MHz, DMSO-*d*₆) δ 164.2, 160.2, 128.8, 122.8, 114.7, 100.8, 61.2, 27.7, 24.5, 18.1. ESI MS (*m/e*) = 238.18 [*M* + 1]⁺.

N,4-dihydroxybenzamide (**6**)

A mixture of compound **5** (0.075 g, 0.49 mmol) in acetonitrile (20 mL) and 3 *N* HCl (10 mL) was stirred at room temperature for 4 h. The mixture was concentrated under reduced pressure and purified by reverse-phase MPLC (SNAP Ultra C18) to afford compound **6** in 10% yield. ¹H NMR (500 MHz, DMSO-*d*₆) δ 7.77 (d, *J* = 8.6 Hz, 1H), 7.60 (d, *J* = 8.6 Hz, 1H), 6.83 (d, *J* = 8.6 Hz, 1H), 6.79 (d, *J* = 9.2 Hz, 1H). ¹³C NMR (125 MHz, DMSO-*d*₆) δ 167.2, 161.6, 131.5, 121.5, 115.1 ESI MS (*m/e*) = 152.04 [*M*-1]⁻.

Docking studies

In silico docking of **4c** with the 3D coordinates of the X-ray crystal structures of HDAC6 (PDB code: 5EF7) was accomplished using the AutoDock program downloaded from the Molecular Graphics Laboratory of the Scripps Research Institute. The AutoDock program was chosen because it uses a genetic algorithm to generate the poses of the ligand inside a known or predicted binding site utilizing the Lamarckian version of the genetic algorithm where the changes in conformations adopted by molecules after in situ optimization are used as subsequent poses for the offspring. In the docking experiments carried out, water was removed from the 3D X-ray coordinates while Gasteiger charges were placed on the X-ray structures of HDAC6 along with **4c** using tools from the AutoDock suite. A grid box centered on the substrate binding pocket of HDAC6 enzyme with definitions of 60_60_60 points and 0.375 Å spacing was chosen for ligand docking experiments. The docking parameters consisted of setting the population size to 150, the number of generations to

27,000, and the number of evaluations to 2,500,000, while the number of docking runs was set to 100 with a cutoff of 1 Å for the root-mean-square tolerance for the grouping of each docking run. The docking model of HDAC6 with compound **4c** was depicted in Fig. 6 and rendering of the picture was generated using PyMol (DeLanoScientific).

Biology

Dulbecco's Modified Eagle's medium (DMEM) with L-glutamine was purchased from GenDEPOT (Barker, TX, USA) and fetal bovine serum (FBS) and penicillin/streptomycin were purchased Gibco BRL (Gaithersburg, MD, USA). Antibodies specific for α-tubulin, Ac-α-tubulin, histone H3, Ac-histone H3, β-actin and Ac-lysine were purchased from Cell Signaling Technology (Boston, MA, USA). Goat anti-rabbit IgG horseradish peroxidase conjugate was purchased from Santa Cruz Biotechnology (Santa Cruz, CA, USA). Cell Titer 96 Aqueous One Solution cell proliferation assay kit was purchased from Promega (Madison, WI, USA). AmershamTM ECL selectTM Western blotting detection reagent was purchased GE Healthcare. HDAC fluorogenic assay kits (HDAC1, HDAC3, HDAC6, and HDAC7) were purchased BPS Bioscience (San Diego, CA, USA).

Cell culture

MDA-MB-231 cells were grown in DMEM with L-glutamine supplemented with streptomycin (500 mg/mL), penicillin (100 units/mL), and 10% fetal bovine serum (FBS). Cells were grown to confluence in a humidified atmosphere (37 °C, 5% CO₂).

Cell proliferation assay

Cell were seeded at 2000 cells per well in a clear 96-well plate, the medium volume was brought to 100 mL, and the cells were allowed to attach overnight. The next day, varying concentrations of **2a-b**, **4b-c**, and **6** or 0.5% DMSO vehicle control were added to the wells. The proliferation of cells was determined using the Promega Cell Titer 96 Aqueous One Solution cell proliferation assay. After incubation with compounds, 20 mL of the assay substrate solution was added to the wells, and the plate was incubated at 37 °C for an additional 1 h. Absorbance at 490 nm was then read on FLUO star[®] Omega (BMG LABTECH), and values were expressed as percent of absorbance from cells incubated in DMSO alone.

Western blot

MDA-MB-231 cells (1×10^6 /dish) were seeded in 50 nm culture dishes, and allowed to attach overnight. Cells were incubated with compound **2a–c**, or compound **4b–c** for an additional 24 h. For comparison, cells were also incubated with 0.5% DMSO. Cells were harvested in ice-cold lysis buffer (23 mM Tris–HCL pH 7.6, 139 mM NaCl, 1% NP-40, 1% sodium deoxycholate, 0.1% SDS), and 30 μ g of lysate per lane was separated by SDS-PAGE and followed by transferring to a PVDF membrane. The membrane was blocked with 5% skim milk in TBS-T, and then incubated with the corresponding antibody. After binding of an appropriated secondary antibody coupled to horseradish peroxidase, proteins were visualized by ECL chemiluminescence according to the instructions of the manufacturer.

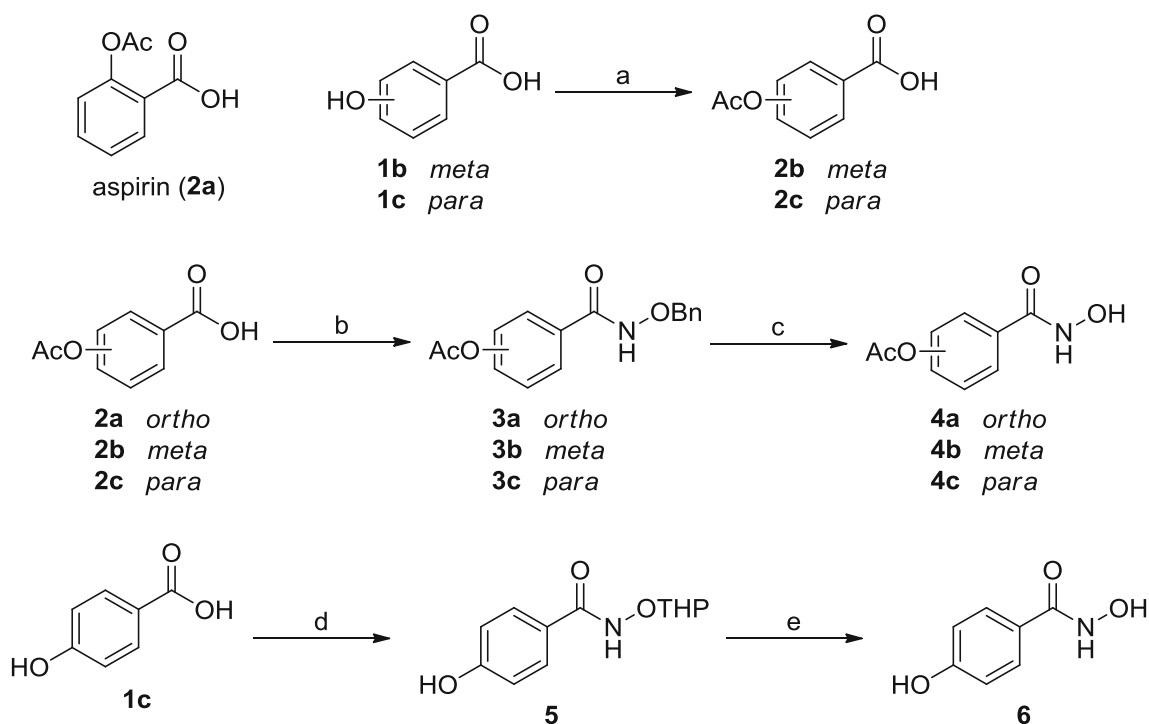
Results

Aspirin analogues **2b–c** were synthesized following the literature procedure with slight modifications (Scheme 1) (Zhang et al. 2014; Hrast et al. 2014). Briefly, compounds **1b–c** were acetylated with acetic anhydride in pyridine to afford **2b–c** in 66–94% yield.

With compounds **2a–c** in hand, we next investigated whether aspirin (**2a**), *meta*-analogue **2b**, and *para*-analogue

2c could promote the acetylation level of lysine ϵ -amino groups in MDA-MB-231 cells. Aspirin is well documented to covalently modify COX-2 through acetylation of Ser530 near its active site and prevents its native substrate from properly binding to its active site (Lei et al. 2015). However, there are only few studies reported about the acetylation capacity of aspirin on lysine residues (Hawkins et al. 1969). Therefore, we measured the acetylating capacity of aspirin (**2a**), *meta*-analogue **2b**, and *para*-analogue **2c** on lysine residues of whole proteins. MDA-MB-231 cells were first treated with aspirin (**2a**), *meta*-analogue **2b**, and *para*-analogue **2c** for 24 h and the acetylation level of lysine residues was assessed by anti-Ac-lysine immunoblot (Fig. 2). Interestingly, aspirin (**2a**) most efficiently promoted the acetylation of lysine residues. Compound **2b** and **2c** were also capable of increasing the acetylation level of lysine residues, compared with DMSO control. Encouraged by the acetylating potential of compounds **2a–c**, we set out to develop a novel acetyl-donating HDAC inhibitors, utilizing the scaffold of compounds **2a–c**.

Most HDAC inhibitors are structurally designed to mimic its endogenous substrate, acetyl-lysine (Fig. 3) (Bassett and Barnett 2014). The common feature of HDAC inhibitor pharmacophore, as exemplified by SAHA, is characterized by three elements, a zinc-binding group (ZBG), a linker, and a cap group. Numerous HDAC inhibitors have been developed to treat a variety of human



Scheme 1 Structure of aspirin and synthesis of aspirin analogue **2b–c**, **4a–c**, and **6**. Reagents and conditions: (a) acetic anhydride, pyridine, rt, 2 h, 94% for **2b**, 66% for **2c**; (b) NH_2OBn , EDC, DIPEA, DCM, rt, 4 h, 71% for **3a**, 68% for **3b**, 60% for **3c**; (c) H_2 , 10% Pd/C, MeOH, rt, 2 h, 45% for **4b**, 39% for **4c**; (d) NH_2OTHP , EDC, DIPEA, DMF, rt, 12 h, 59%; (e) 3 N HCl, MeCN, rt, 4 h, 10%

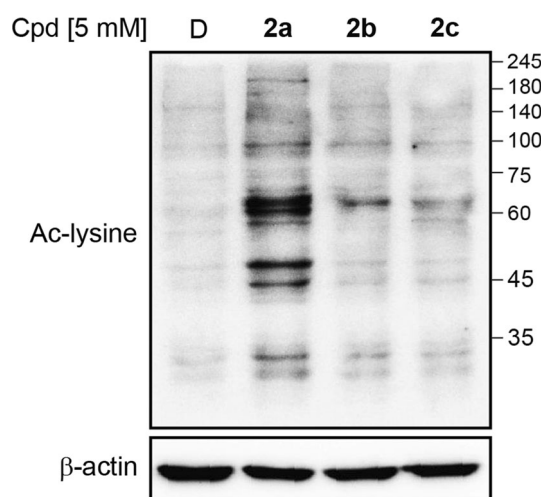


Fig. 2 Comparative acetylating capacity of aspirin (**2a**), *meta*-analogue **2b**, and *para*-analogue **2c** on lysine residues. MDA-MB-231 cells were treated with 5 mM of the indicated compound for 24 h and the effect of compound **2a**, **2b**, and **2c** on the acetylation status of whole proteins was analyzed by western blot. DMSO (D) was used as a negative control

diseases and the majority of these HDAC inhibitors incorporate hydroxamic acid as a zinc-binding group, including clinically approved SAHA, PXD101, and LBH589 (Bassett and Barnett 2014). At the same time, the phenyl linker of HDAC inhibitors has been widely used in the development of HDAC inhibitors due to its hydrophobic nature, well fitting into the lipophilic channel of HDAC substrate pocket. Accordingly, we designed new HDAC inhibitors by installing a hydroxamic acid zinc-binding group and a phenyl linker to the structures of

aspirin, *meta*-analogue **2b**, and *para*-analogue **2c**, leading to acetyl-donating HDAC inhibitors shown in Fig. 3.

The synthesis of acetyl-donating HDAC inhibitors **4a–c** is summarized in Scheme 1. We first carried out EDC-mediated amide coupling of compound **2a–c** with NH_2OBn in the presence of DIPEA to provide benzyl-protected compound **3a–c** in 60–71% yield. The removal of benzyl-protecting group under hydrogen atmosphere in the presence of 10% palladium catalyst successfully furnished compound **4b–c** in 39–45% yield. Unfortunately, the attempt to cleave benzyl-protecting group from **3a** under the same reaction condition did not lead to a fruitful result. It only provided a complex mixture, indicating compound **4a** was not stable and decomposed upon the removal of protecting group unlike other analogues (**4b–c**).

To clarify the mode of action of acetyl donating HDAC inhibitor, we aimed at the synthesis of compound **6** that lacks acetyl-donating group. The synthesis began with the coupling reaction of **1c** with NH_2OTHP in the presence of EDC and DIPEA in DMF, providing compound **5** in 59% yield. Acidic cleavage of THP-protecting group from compound **5** using 3 N HCl in acetonitrile successfully furnished compound **6** in 10% yield.

Upon completion of synthesis, we evaluated the anti-proliferative activity of compound **2a–c**, **4b–c**, and **6** against MDA-MB-231 cell line, which is a highly aggressive and invasive triple-negative breast cancer (TNBC) cell line. It lacks estrogen receptor (ER), progesterone receptor (PR), and human epidermal growth factor receptor (Her2). As shown in Table 1, compound **2a** (aspirin), **2b**, and **2c** exhibited very poor anti-proliferative activities against

Fig. 3 Design of acetyl-donating HDAC inhibitors. ADG, acetyl-donating group; ZBG, zinc-binding group

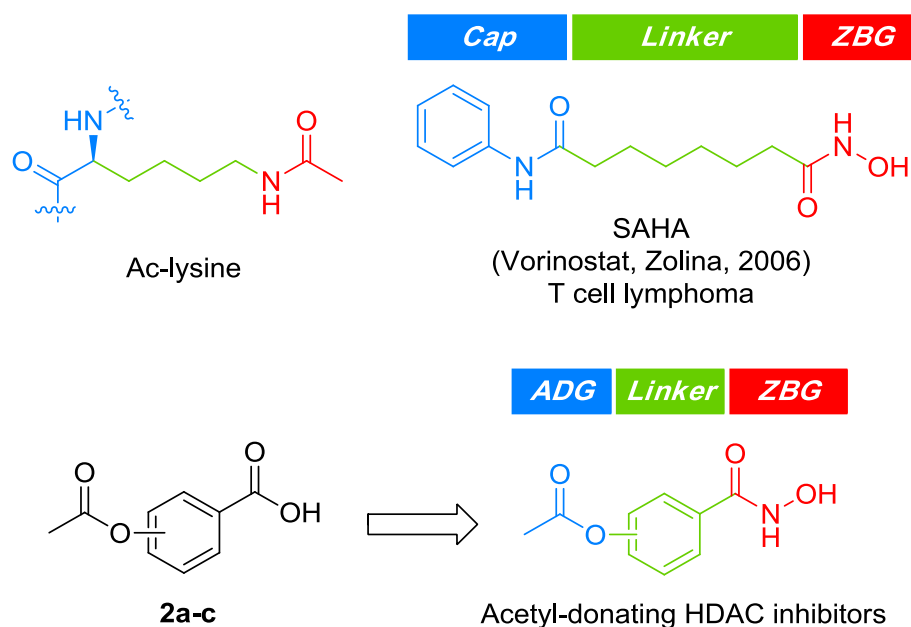
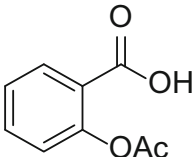
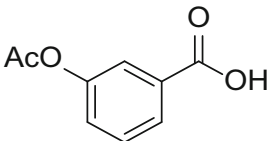
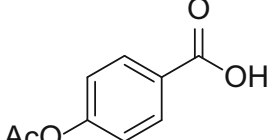
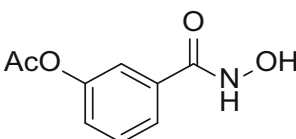
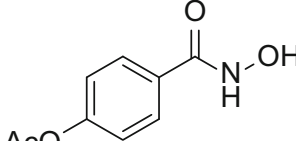
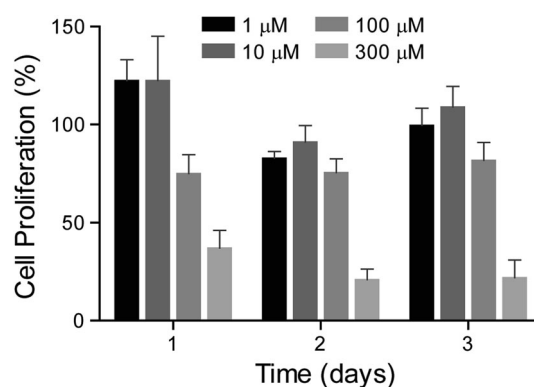


Table 1 Anti-proliferative effect of compound **2a–c**, **4b–c**, and **6** against breast cancer cell line, MDA-MB-231

Compound	Structure	MDA-MB-231 (GI ₅₀ ; μM)
2a (aspirin)		> 1000
2b		720
2c		> 1000
4b		169
4c		147
6		554

MDA-MB-231 TNBC cell line, in that GI₅₀ values of compound **2a** and **2c** were higher than 1,000 μM and GI₅₀ value of compound **2b** was 720 μM. As expected, compound **4b** and **4c** displayed a significantly improved anticancer effect against MDA-MB-231 cell line with GI₅₀ values of 169 μM and 147 μM, compared with their parent compound **2b** and **2c**. Interestingly enough, compound **6** that lacks acetyl-donating group (ADG) demonstrated a relatively poor anticancer effect (GI₅₀ = 554 μM), compared with compound **4c** (GI₅₀ = 147 μM), clearly indicating that acetyl-donating group of compound **4c** played an important role in anticancer effect. Overall, the result strongly validates molecular design of acetyl-donating HDAC inhibitors in the discovery of novel HDAC inhibitors.

To examine time- and dose-dependent effect of compound **4c** on the growth of MDA-MB-231 cells, we treated MDA-MB-231 cells with compound **4c** at various concentration (1, 10, 100, and 300 μM) for 1, 2, and 3 days and measured the cell proliferation using MTS assay (Fig. 4). The cell proliferation assay indicated that compound **4c** afforded relatively good cellular efficacy against MDA-MB-231 cells in a dose-dependent manner. The

**Fig. 4** Time- and dose-dependent anti-proliferative effect of **4c** on MDA-MB-231 cells

exposure of cells with 300 μM of compound **4c** displayed a significant anticancer effect and impaired the growth of MDA-MB-231 cells by 37, 21, and 22% for 1, 2, and 3 days, respectively.

We next assessed the comparative effect of aspirin, **4c**, and **4b** on the acetylation status of α-tubulin and histone H3, which were epigenetically removed by HDAC6 and HDAC1 enzymes, respectively. As shown in Fig. 5, the

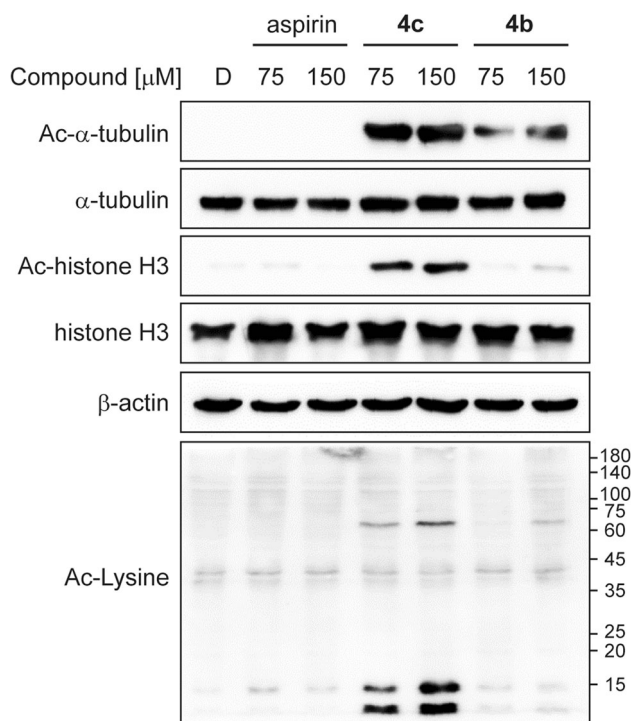


Fig. 5 Comparative effect of aspirin, **4c**, and **4b** on the acetylation status of α -tubulin and histone H3. MDA-MB-231 cells were treated with 75 or 150 μM of aspirin, **4c**, and **4b** for 24 h and the expression of the indicated proteins was determined by western blot. DMSO (D) was employed as a negative control

treatment of MDA-MB-231 cells with compound **4c** significantly promoted the acetylation of α -tubulin and histone H3, while the reference drug, aspirin failed to induce the acetylation of α -tubulin and histone H3. Compound **4b** was less effective on acetylating α -tubulin than compound **4c**, and incapable of acetylating histone H3. As expected, the expression level of α -tubulin and histone H3 remain unaffected by aspirin, **4c**, and **4b**. We next measured the total acetylation status of whole proteins in MDA-MD-231 cells. Compound **4c** acetylated ϵ -amino group of lysine residues more efficiently than the reference drug aspirin and the other analogue **4b**, evidenced by anti-Ac-lysine immunoblot. Taken together, the result clearly demonstrated that *para*-analogue **4c** most significantly inhibited HDAC1 and HDAC6 enzymes and promoted the acetylation of their substrates, histone H3 and α -tubulin, respectively.

To assess the precise binding pose of compound **4c** to HDAC6, we carried out in silico docking simulation of compound **4c** into the substrate binding pocket of HDAC6 (PDB code: 5EF7). As shown in Fig. 6, the docking simulation indicated that compound **4c** nicely occupied the deep substrate binding pocket of HDAC6. *Para*-acetyl group of compound **4c** was located in the rim of the substrate binding pocket and the carbonyl oxygen (C=O) of the

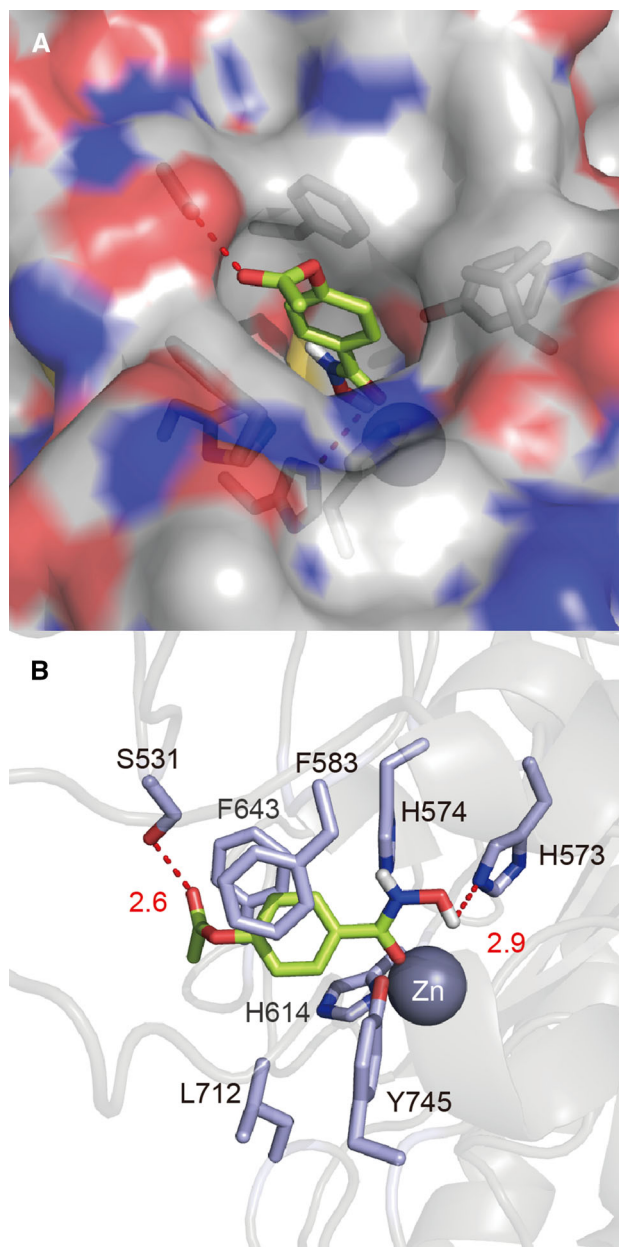


Fig. 6 Molecular docking model of **4c** in the binding pocket of HDAC6 (PDB code: 5EF7)

acetyl group formed a hydrogen bond interaction with S531 residue. The phenyl ring of **4c** projected into the lipophilic channel of HDAC6, forming π - π interactions with F583 and F643 residues. The hydroxamate OH and C=O groups of compound **4c** coordinated the active site Zn^{2+} ion in a bidentate manner. Additionally, the hydroxamate OH group of **4c** participated in a hydrogen bond interaction with H573 residue.

Discussion

With the aim of generating acetyl-donating HDAC inhibitors, we designed, synthesized, and performed biological evaluation of a series of aspirin derivatives. The results revealed that aspirin (**2a**), together with its *meta*-analogue **2b** and *para*-analogue **2c** was able to promote the acetylation of lysine residues, establishing the proof of principle for the strategy of developing acetyl-donating HDAC inhibitors. By virtue of aspirin's acetylating potential, we developed novel acetyl-donating HDAC inhibitors by modifying the scaffold of compound **2a–c**. The biological evaluation clearly indicated that compound **4c** ($GI_{50} = 147 \mu\text{M}$) afforded the significant enhancement of anti-cancer effect on TNBC MDA-MB-231 cells, compared with its parent compound **2c** ($GI_{50} > 1,000 \mu\text{M}$) and ADG-deficient analogue **6** ($GI_{50} = 554 \mu\text{M}$). The treatment of MDA-MB-231 cells with compound **4c** significantly promoted the acetylation of α -tubulin and histone H3, which are substrates of HDAC6 and HDAC1, respectively. Moreover, the docking simulation demonstrated that compound **4c** tightly bound to the deep substrate-binding pocket of HDAC6 by coordinating the active Zn^{2+} ion in a bidentate fashion and forming hydrogen bond interactions with amino acid residues. Overall, this study for the first time demonstrated the design, synthesis, and biological evaluation of acetyl-donating HDAC inhibitors and presented the novel strategy for developing acetyl-donating HDAC inhibitors.

Acknowledgements This research was supported by Basic Science Research Program through the National Research Foundation of Korea (NRF) funded by the Ministry of Education (NRF-2016R1A6A1A03011325 and 2016R1D1A1B01009559), and Korea Institute of Planning and Evaluation for Technology in Food, Agriculture, Forestry and Fisheries (IPET) through Animal Disease Management Technology Development Program, funded by the Ministry of Agriculture, Food and Rural Affairs (MAFRA) (116102-03).

Compliance with ethical standards

Conflict of interest The authors declare no conflict of interest.

References

- Bassett SA, Barnett MP (2014) The role of dietary histone deacetylases (HDACs) inhibitors in health and disease. *Nutrients* 6:4273–4301
- Bolden JE, Peart MJ, Johnstone RW (2006) Anticancer activities of histone deacetylase inhibitors. *Nat Rev Drug Discov* 5:769–784
- Chun P (2018) Therapeutic effects of histone deacetylase inhibitors on kidney disease. *Arch Pharm Res* 41:162–183
- Cuadrado-Tejedor M, Garcia-Barroso C, Sanchez-Arias JA, Rabal O, Perez-Gonzalez M, Mederos S, Ugarte A, Franco R, Segura V, Perea G, Oyarzabal J, Garcia-Osta A (2017) A first-in-class small-molecule that acts as a dual inhibitor of HDAC and PDE5 and that rescues hippocampal synaptic impairment in Alzheimer's disease mice. *Neuropsychopharmacology* 42:524–539
- D'yedwalle C, Bogaert E, Van Den Bosch L (2012) HDAC6 at the intersection of neuroprotection and neurodegeneration. *Traffic* 13:771–779
- Duvic M, Talpur R, Ni X, Zhang C, Hazarika P, Kelly C, Chiao JH, Reilly JF, Ricker JL, Richon VM, Frankel SR (2007) Phase 2 trial of oral vorinostat (suberoylanilide hydroxamic acid, SAHA) for refractory cutaneous T-cell lymphoma (CTCL). *Blood* 109:31–39
- Glozak MA, Sengupta N, Zhang X, Seto E (2005) Acetylation and deacetylation of non-histone proteins. *Gene* 363:15–23
- Golden SA, Christoffel DJ, Heshmati M, Hodes GE, Magida J, Davis K, Cahill ME, Dias C, Ribeiro E, Ables JL, Kennedy PJ, Robison AJ, Gonzalez-Maeso J, Neve RL, Turecki G, Ghose S, Tamminga CA, Russo SJ (2013) Epigenetic regulation of RAC1 induces synaptic remodeling in stress disorders and depression. *Nat Med* 19:337–344
- Hawkins D, Pinckard RN, Crawford IP, Farr RS (1969) Structural changes in human serum albumin induced by ingestion of acetylsalicylic acid. *J Clin Invest* 48:536–542
- Hong L, Schroth GP, Matthews HR, Yau P, Bradbury EM (1993) Studies of the DNA binding properties of histone H4 amino terminus. Thermal denaturation studies reveal that acetylation markedly reduces the binding constant of the H4 "tail" to DNA. *J Biol Chem* 268:305–314
- Hrast M, Anderlüh M, Knez D, Randall CP, Barretheau H, O'Neill AJ, Blanot D, Gobec S (2014) Design, synthesis and evaluation of second generation MurF inhibitors based on a cyanothiophene scaffold. *Eur J Med Chem* 73:83–96
- Kazantsev AG, Thompson LM (2008) Therapeutic application of histone deacetylase inhibitors for central nervous system disorders. *Nat Rev Drug Discov* 7:854–868
- Lee DY, Hayes JJ, Pruss D, Wolffe AP (1993) A positive role for histone acetylation in transcription factor access to nucleosomal DNA. *Cell* 72:73–84
- Lee HZ, Kwitkowski VE, Del Valle PL, Ricci MS, Saber H, Habtemariam BA, Bullock J, Bloomquist E, Li Shen Y, Chen XH, Brown J, Mehrotra N, Dorff S, Charlab R, Kane RC, Kaminskas E, Justice R, Farrell AT, Pazdur R (2015) FDA approval: belinostat for the treatment of patients with relapsed or refractory peripheral T-cell lymphoma. *Clin Cancer Res* 21:2666–2670
- Lei J, Zhou Y, Xie D, Zhang Y (2015) Mechanistic insights into a classic wonder drug—aspirin. *J Am Chem Soc* 137:70–73
- Lu X, Ning Z, Li Z, Cao H, Wang X (2016) Development of chidamide for peripheral T-cell lymphoma, the first orphan drug approved in China. *Intractable Rare Dis Res* 5:185–191
- Nebbioso A, Carafa V, Benedetti R, Altucci L (2012) Trials with 'epigenetic' drugs: an update. *Mol Oncol* 6:657–682
- Omonijo O, Wongprayoon P, Ladenheim B, McCoy MT, Govitrapong P, Jayanthi S, Cadet JL (2014) Differential effects of binge methamphetamine injections on the mRNA expression of histone deacetylases (HDACs) in the rat striatum. *Neurotoxicology* 45:178–184
- Patrignani P, Patrono C (2016) Aspirin and cancer. *J Am Coll Cardiol* 68:967–976
- Raedler LA (2016) Farydak (Panobinostat): first HDAC inhibitor approved for patients with relapsed multiple myeloma. *Am Health Drug Benefits* 9:84–87
- Ropero S, Esteller M (2007) The role of histone deacetylases (HDACs) in human cancer. *Mol Oncol* 1:19–25
- Sonnemann J, Huls I, Sigler M, Palani CD, Le Hong TT, Volker U, Kroemer HK, Beck JF (2008) Histone deacetylase inhibitors and

- aspirin interact synergistically to induce cell death in ovarian cancer cells. *Oncol Rep* 20:219–224
- Tambaro FP, Dell'aversana C, Carafa V, Nebbioso A, Radic B, Ferrara F, Altucci L (2010) Histone deacetylase inhibitors: clinical implications for hematological malignancies. *Clin Epigenetics* 1:25–44
- Vandermolen KM, Mcculloch W, Pearce CJ, Oberlies NH (2011) Romidepsin (Istodax, NSC 630176, FR901228, FK228, depsipeptide): a natural product recently approved for cutaneous T-cell lymphoma. *J Antibiot (Tokyo)* 64:525–531
- Zhang YJ, Shen LL, Cheon HG, Xu YN, Jeong JH (2014) Synthesis and biological evaluation of glucagon-like peptide-1 receptor agonists. *Arch Pharm Res* 37:588–599